

Langmuir probe measurements in an expanding magnetized plasma

G. J. H. Brussaard,¹ M. van der Steen,¹ M. Carrère,² M. C. M. van de Sanden,¹ and D. C. Schram¹
¹*Department of Physics, Eindhoven University of Technology, P.O. Box 513, 5600 MB Eindhoven, The Netherlands*
²*Equipe Plasma Surface, Université de Saint Jerome, Case 232, 13341 Marseille Cedex 20, France*

(Received 21 February 1996)

Langmuir probe measurements are performed in magnetized expanding plasmas of different compositions. The influence of the magnetic field on the currents collected by the probe in an argon plasma is investigated at two different flows and for two different probe sizes. The experimental results are compared to existing theories. A decrease in the ratio of electron to ion saturation currents is found both in theory and experimentally. However, the theoretically predicted dependence of the ratio of electron to ion saturation current on probe diameter is not observed. An empirically derived function is fitted to the data. Under the assumption that the function fitted to the results in argon is valid in other plasmas, it is possible to determine relative ion densities in magnetized nitrogen and hydrogen plasmas. It is found that the dominant ionic species in both plasmas is the atomic ion (N^+ and H^+ , respectively). [S1063-651X(96)08008-7]

PACS number(s): 52.70.-m, 52.40.Hf

I. INTRODUCTION

Expanding plasmas have become increasingly interesting for application to a wide variety of technologies. As a hydrogen particle source they are used for surface modification, passivation, and plasma cleaning of iron archaeological artifacts [1]. The argon hydrogen plasma serves as a precursor to deposition plasmas that are used for fast deposition of amorphous hydrogenated silicon ($a\text{-Si:H}$), amorphous carbon ($a\text{-C:H}$), diamond, and silicon nitride (SiN_x) layers [2–4]. The nitrogen plasma has applications to surface treatment by nitriding to realize hard anticorrosive layers such as titanium nitride (TiN), and is of fundamental interest in the study of N_2/O_2 mixtures for the understanding of reentry problems with spacecraft.

To investigate two of the principal characteristics of a plasma, the ionization degree and temperature of the plasma, the static Langmuir probe is one of the most widely used techniques. However, the theory of such probes under non-ideal circumstances, such as the application of a magnetic field, is still a topic of much research. In this paper we will investigate the effect of a magnetic field on Langmuir probe characteristics for several different plasma conditions and compositions and the applicability of the existing theory.

II. EXPERIMENTS

A. Cascaded arc plasma

The plasma source used is the cascaded arc [Fig. 1(a)], with three cathodes, a stack of four isolated copper plates with a 4-mm bore, and an anode nozzle. The current can be varied, but is set to 50 A in the experiments described here. The voltage drop depends on the gas flow rate and gas composition and ranges from 50–100 V. Details of the operation of the cascaded arc can be found in [5]. The gas is injected at the cathode side and is dissociated and ionized in the arc channel. The plasma is then allowed to expand supersonically into a low-pressure chamber [Fig. 1(b)].

The ion density at larger distances from the nozzle can be increased by applying a magnetic field. For this purpose a

coil around the nozzle provides a diverging magnetic field downstream that is parallel to the plasma flow with a maximum field strength of 40 mT. An overview of all relevant parameters during the experiments is given in Table I.

B. Planar probe

For the investigation of the electron temperature and density of the plasma, two planar probes were constructed. The probes [Fig. 2(a)] are circular probes made out of tungsten. A

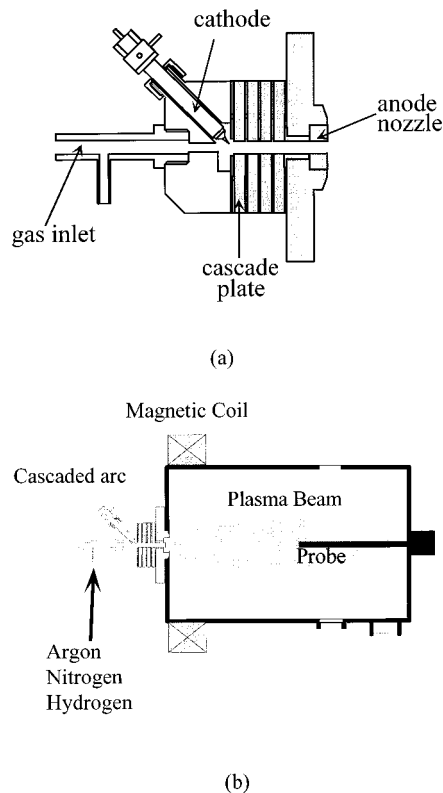


FIG. 1. Cascaded arc plasma source (a) and the expanding plasma setup (b).

TABLE I. Overview of experimental conditions.

Ar flow	0.3 and 1 slm
N ₂ flow	1.4 slm
H ₂ flow	2 slm
Arc current	50 A
Chamber pressure	10–30 Pa
Magnetic field	0–18 mT

probe with a diameter of 4 mm and one with a diameter of 1.8 mm were used. The edges of the probe are shielded off by a ceramic (Al₂O₃) tube. Although it has been argued by Schott [6] that the charge collected on the tube will distort the field in front of the probe in an uncontrollable way, this is thought not to be of great influence on the plasmas under investigation here, because the electron density in the plasmas under investigation is of the order of 10^{17} – 10^{18} m⁻³ and

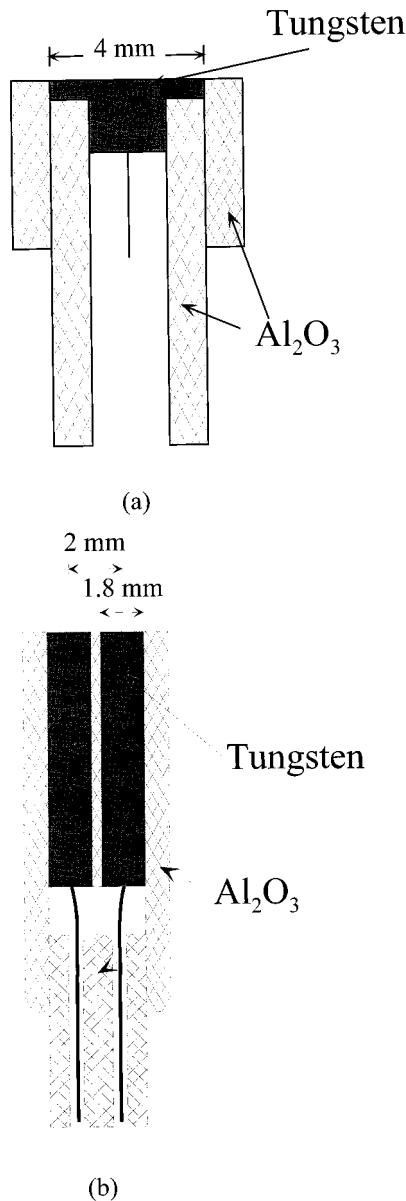


FIG. 2. Single (a) and double (b) Langmuir probes.

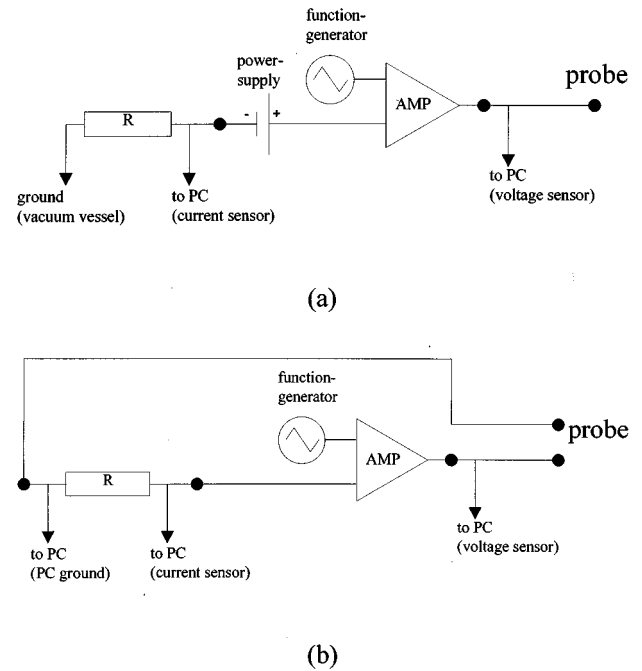


FIG. 3. Electrical circuit for measurements with the single probe (a) and double probe (b).

the temperature is 0.1–0.5 eV. The Debye length consequently is of the order of 10^{-5} m. The distortion of the field by the ceramic tube will therefore be limited to an area much smaller than the probe area. An advantage of this design is that no edge effects need be taken into account. Furthermore, it is possible to use this probe in combination with a laser in photoionization and photodetachment experiments [7] without exposing the probe surface to the laser beam.

The probe is placed inside the plasma at a distance of 25 cm from the nozzle for argon and nitrogen and 16 cm for hydrogen. The normal to the probe surface is parallel to the flow and the applied magnetic field. The current collected by the probe is measured as a function of the applied potential relative to ground. A schematic overview of the circuit is given in Fig. 3(a).

For double probe measurements, a similar probe design was used [Fig. 2(b)]. The probe consists of two circular tungsten disks (diameter 1.8 mm) mounted inside a ceramic tube, 2 mm apart. In this setup the current through the probe is measured as a function of applied potential difference. The complete setup is therefore floating with respect to ground. An overview of the setup is given in Fig. 3(b).

III. THEORY

A. Single planar probe

In the experiments described, the single planar probe is immersed in a plasma and the current is measured as a function of the applied potential. If a large positive potential is applied, the current drawn from the plasma to the probe saturates. The electron current is then limited to the random flux of electrons in the sheath around the probe. As was shown in the Sec. II B, the Debye length in the plasma is very small (of the order of 10^{-5} m) compared to the probe diameter.

The collection surface, consequently, can be taken to be equal to the actual probe surface A_p . If no magnetic field is applied, the mean-free path of the electrons is in the range of 0.5 mm, for argon, to 7 mm, for hydrogen, i.e., much larger than the thickness of the sheath and of the order of the probe radius. For this case the electron saturation current I_s is given by [8]

$$I_{es} = -\frac{1}{4}n_{e0}\bar{v}_e e A_p, \quad (1)$$

with n_{e0} the electron density of the undisturbed plasma, \bar{v}_e the electrons' mean velocity, and e the electron charge. A Maxwellian velocity distribution is assumed so that $\bar{v}_e = \sqrt{(8/\pi)(kT_e/m_e)}$, with T_e the electron temperature and k Boltzmann's constant.

In the expanding plasma the ion temperature T_i is approximately equal to the electron temperature. It was shown by Laframboise [9] that in this case ($T_i \approx T_e$) ion collection does not differ from electron collection and no so-called presheath [10] is present. The ion saturation current I_{+s} , at high negative potentials, is then given by an expression very similar to (1) and the ratio between electron and ion saturation current becomes

$$\frac{I_{es}}{I_{+s}} = \sqrt{\frac{m_+}{m_e}}, \quad (2)$$

which is 270 for argon.

B. Single planar probe in a strong magnetic field

The situation is considerably more complicated if a magnetic field is applied. When the magnetic field is sufficiently strong, the electrons will be confined to the magnetic field lines. The electron current collected by the probe will, due to this confinement, be reduced. Although there have been several theoretical studies [10–12], there is still no consistent theory to fully explain the reduction. Most widely used is the theory of Bohm *et al.* [10].

When a magnetic field is applied, the electrons will be forced into a circular motion with a radius ρ_e equal to the Larmor radius

$$\rho_e = \frac{m_e \bar{v}_e}{eB}, \quad (3)$$

with B the applied magnetic field. If the Larmor radius becomes smaller than the mean-free path of the electron ($\rho_e < \lambda$), the plasma is effectively confined. If, under these conditions, the Larmor radius is also smaller than the dimensions perpendicular to the magnetic field of the probe ($\rho_e < r_p$, in the case of a planar probe with the normal of its surface parallel to the magnetic field), the current to the probe is limited by diffusion. The particle flux to the probe in this case is given by

$$\vec{\Gamma} = -\underline{D} \cdot \vec{\nabla} n - n \underline{\mu} \cdot \vec{\nabla} V. \quad (4)$$

The diffusivity \underline{D} and the mobility $\underline{\mu}$ are anisotropic, due to the magnetic field. The diffusion along the magnetic-field

lines remains unchanged ($D_e = \frac{1}{3}\lambda\bar{v}$), but the components perpendicular to the direction of the magnetic field D_{\perp} are reduced:

$$D_{e\perp} = \frac{D_e}{1 + (\lambda/\rho_e)^2}. \quad (5)$$

It is assumed that Einstein's relation $\mu = eD/kT$ is still valid. For a planar, circular probe with the normal of its surface parallel to the magnetic field, the electron saturation current then becomes [13]

$$I_{e\parallel} = I_0 \beta, \quad (6)$$

with I_0 the undisturbed, random current given by Eq. (1) and a reduction $\beta(B)$ due to the magnetic field of

$$\beta = \left(1 + \frac{\pi}{8} \frac{r_p}{\lambda} [1 + (\lambda/\rho_e)^2]^{1/2} \right)^{-1}. \quad (7)$$

The ratio of saturation currents becomes

$$\frac{I_{es\parallel}}{I_{+s}} = \sqrt{\frac{m_+}{m_e}} \beta. \quad (8)$$

C. Double Langmuir probe [14]

The saturation current to a floating double probe is given by [similar to Eq. (1)]:

$$I_{+s1,2} = \pm \frac{1}{4}n_{+0}\bar{v}_+ q_+ A_{p1,2}, \quad (9)$$

with $A_{p1,2}$ the surface area of the probe considered and q_+ the charge of the ion. For small potentials current is also carried by the electrons and the current through the probes is given by

$$\begin{aligned} I_p &= I_{e1} - I_{+s1} = I_{es1} e^{eV_1/kT_e} - I_{+s1} \quad (V_p < 0), \\ I_p &= I_{+s2} - I_{e2} = I_{+s2} - I_{es2} e^{eV_1/kT_e} \quad (V_p > 0). \end{aligned} \quad (10)$$

After rearranging Eq. (10) to

$$\frac{I_p - I_{+s1}}{I_{+s2} - I_p} = \frac{A_{p1}}{A_{p2}} e^{eV_p/kT_e}, \quad (11)$$

the electron temperature is obtained. Because $T_i \approx T_e$, the ion (electron) density can be calculated from Eq. (9). It is easily seen, by inserting the electron current from Eq. (6) into Eq. (10), that the presence of a magnetic field does not change the characteristics of the double probe [Eq. (11)].

IV. ARGON PLASMA

To check the validity and applicability of the theory, measurements were performed in a pure argon plasma at two different flows [0.3 and 1 slm]. The pumping speed was kept constant, resulting in chamber pressures of 11 Pa at 0.3-slm flow and 27 Pa at 1 slm. The two probes as described in Sec. II were placed with the normal of their surfaces parallel to the magnetic field at a distance of 24 cm from the nozzle. Measurements were made at magnetic fields between 0 and 16 mT. The probe characteristics at different magnetic fields

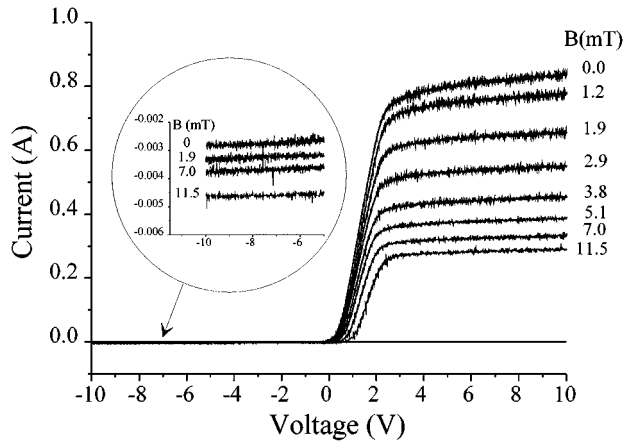


FIG. 4. Single probe characteristics at different magnetic fields, measured with a 4-mm-probe diameter, in an argon flow of 1 slm. The enlargement shows the development of ion saturation current with magnetic field.

at an argon flow of 0.3 slm, measured by the larger probe (4-mm diameter) are shown in Fig. 4. The electron densities and temperatures measured by the double probe are shown in Fig. 5. The ratio of electron to ion saturation currents as a function of the magnetic field for flows of 0.3 and 1 slm is shown in Figs. 6(a) and 7(a), respectively. The same ratios are shown as a function of the Hall parameter λ/ρ_e in Figs. 6(b) and 7(b).

It was found that the current ratios in the absence of a magnetic field range between 290 and 350. The theory of a probe with a collisionless sheath as described in the Sec. III A predicts a value of 270. The mean-free path for electron-ion collisions is 1.6 mm at 0.3-slm flow (11 Pa) and 0.3 mm at 1-slm flow (27 Pa). The mean-free path for collisions with neutral particles is much larger (>2 cm at $p=27$ Pa, $T_e=0.25$ eV). The Debye length is of the order of 10^{-6} m in both plasmas. Under these conditions the assumption of a collisionless sheath can be made. The discrepancy between the theoretically predicted ratio of electron to ion saturation current of 270 and the experimental result of 290 ± 30 is pos-

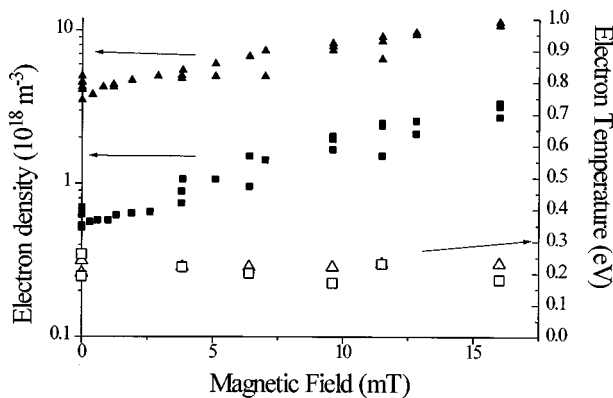
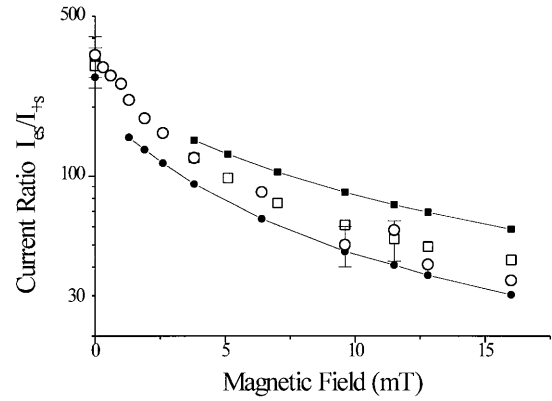
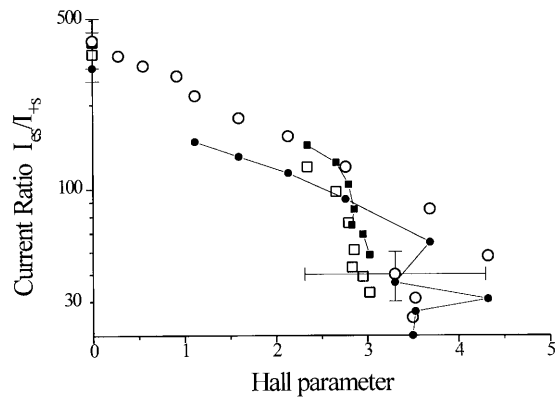


FIG. 5. Electron density and electron temperature measured by the Langmuir double probe. Squares are measurements in a flow of 0.3 slm (\blacksquare , n_e ; \square , T_e), triangles are results in a flow of 1 slm (\blacktriangle , n_e ; \triangle , T_e).



(a)



(b)

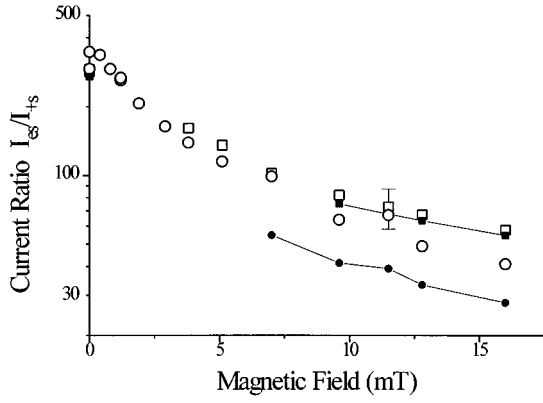
FIG. 6. Current ratio as a function of magnetic field (a) and as a function of the Hall parameter (b) in an argon plasma with a total flow of 0.3 slm. The circles (\circ , measurements; \bullet , calculations) are results with a 1.8-mm-probe diameter. The squares (\square , measurements; \blacksquare , calculations) are results with a 4-mm-probe diameter.

sibly caused by the probe geometry.

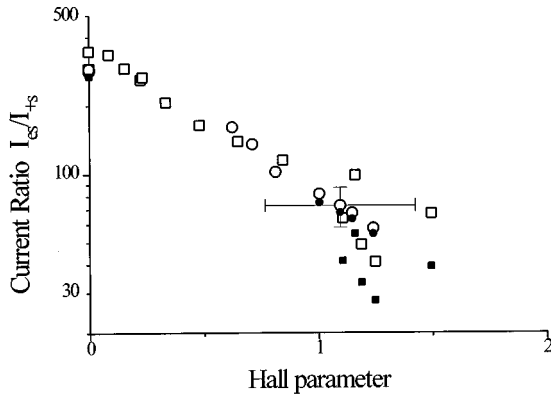
With electron temperature and density measured by the double probe as input parameters, Eq. (8) was used to calculate the ratio of electron to ion saturation current at different values of the magnetic field. The results of these calculations are also shown in Figs. 6 and 7. In the case of the higher (1 slm) argon flow (Fig. 7), confinement is reached at a higher magnetic field, due to the smaller mean-free path caused by a higher electron (ion) density. Therefore Eq. (8) becomes valid at higher magnetic fields. The theoretical values at $B=0$ are calculated using Eq. (2).

It can be seen in these figures that there is qualitative agreement between theory and the experiments performed. The dependence on probe radius as predicted in Eq. (7) is not observed for either of the two flows. A possible explanation may be found in the fact that the flow of the plasma was neglected in the derivation of the equations. Also, the ceramic tubes around the probe will influence the flow pattern near the probes.

In order to be able to describe the dependency of the



(a)



(b)

FIG. 7. Measurements and calculations in an argon plasma with a total flow of 1 slm. The symbols are equivalent to those of Figs. 6(a) and 6(b).

current ratio on the applied magnetic field empirically, the probe ratio dependency was removed from Eq. (7). A variable l is now introduced as a fitting parameter:

$$\beta^* = \left(1 + \frac{\pi l}{8 \lambda} [1 + (\lambda/\rho_e)^2]^{1/2} \right)^{-1}. \quad (12)$$

The best fit is obtained with $l = 1.2 \pm 0.2$ mm. Using this value the difference between theory and measurements is less than 20% for both flows and both probe radii.

V. NITROGEN

If it is assumed that the empirically derived equation [Eq. (12)] and value for l are also valid for gases other than argon, it is possible to use the probe in the investigation of other, more complicated, magnetized plasmas. One of the plasmas of interest in surface modification and deposition studies is the nitrogen plasma. For the investigation the setup described in Sec. II was used. A pure nitrogen plasma was created with a total flow of 1.4 slm at a pressure inside the vessel of 23 Pa. The electron densities vary between $0.7 \times 10^{17} \text{ m}^{-3}$ at

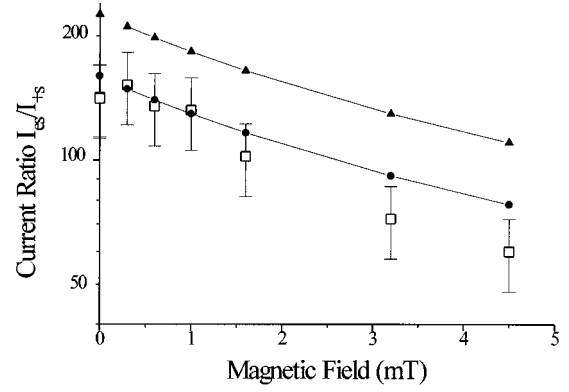


FIG. 8. Results from the nitrogen plasma with a total flow of 1.4 slm. The open symbols (\square) are measured values. The solid symbols are results from calculations assuming that all ions are N^+ (\bullet) and N_2^+ (\blacktriangle), respectively.

$B=0$ and $5 \times 10^{17} \text{ m}^{-3}$ at $B=4.5$ mT. The measured ratios of saturation currents at different values of the magnetic field are shown in Fig. 8. Because nitrogen forms two possible ions (N^+ and N_2^+) the current ratio will be determined by the relative densities of these ions:

$$\frac{I_{es}}{I_{+s}} = \sqrt{\frac{m_{\text{N}^+} \left(\frac{n_{\text{N}^+} + 2n_{\text{N}_2^+}}{n_+} \right)}{m_e}} \beta^* \quad (13)$$

with n_{N^+} and $n_{\text{N}_2^+}$ the N^+ and N_2^+ densities, and n_+ the total ion density. In Fig. 5 the calculated current ratios are given for two distinct cases: $n_{\text{N}^+}/n_+ = 1$ and $n_{\text{N}^+}/n_+ = 0$. It is clear that a best fit would yield $n_{\text{N}^+}/n_+ = 1$. Taking into account the accuracy derived in Sec. IV, it is possible to conclude that in this magnetized plasma the atomic ion N^+ is the dominant ionic species. This result is in agreement with mass spectrometry measurements performed by Dahiya *et al.* [15]. Simple kinetic considerations can be used to understand this result: Due to the high energy density inside the arc, N^+ will be the dominant ion at the nozzle. Any N_2^+ that might be produced downstream will be quickly destroyed, because the destruction of N_2^+ through the dissociative recombination $\text{N}_2^+ + e^- \rightarrow 2\text{N}$ is far more efficient than the three-particle recombination $\text{N}^+ + e + M \rightarrow \text{N} + M$ needed to neutralize N^+ . N^+ is therefore likely to be the dominant ion downstream in the plasma.

VI. HYDROGEN

An even more complex plasma is the hydrogen plasma. Hydrogen is known to form many different ions H^+ , H_2^+ , H_3^+ , and even larger ionic molecules [16]. Besides these positive ions, the negative ion H^- is also stable. This makes it impossible to make a full quantitative analysis of the distribution of the charged particles in hydrogen using the method described. However, some qualitative conclusions can be drawn from an investigation of the saturation currents.

In Fig. 9 the saturation current ratio in a pure hydrogen plasma, at a distance of 16 cm from the nozzle, at a flow rate of 2 slm and a chamber pressure of 23 Pa, is shown as a

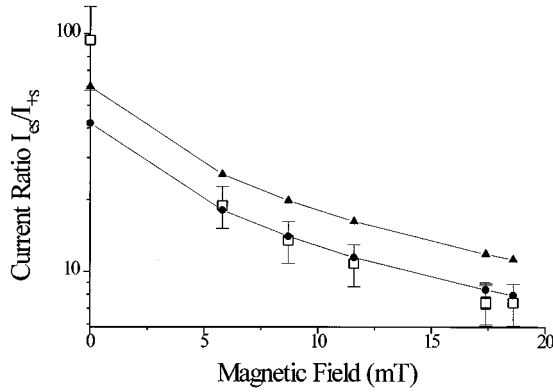


FIG. 9. Results from the hydrogen plasma with a total flow of 2 slm. The open symbols (\square) are measured values. The solid symbols are results from calculations assuming that all ions are H^+ (\bullet) and H_2^+ (\blacktriangle), respectively.

function of the magnetic field. The electron densities vary between $0.1 \times 10^{17} \text{ m}^{-3}$ and $14 \times 10^{17} \text{ m}^{-3}$ for magnetic fields between 0 and 18 mT. Without going fully into the theories that exist about probe analysis in the presence of negative ions [17], it is possible to estimate from the current ratios whether or not H^- is the dominant negative particle. Because of the difference in mobility between electrons and H^- , the density of H^- needs to be a factor of 10 higher than the electron density for the ion to be the dominant negative particle. If H^- would be the dominant negative particle, the saturation current at $B=0$ would be between 1 and 2, depending on the distribution of positive-ion densities (H^-/H^+ would yield a current ratio of 1; H^-/H_3^+ would yield 1.7). At increased magnetic field this ratio would remain within this region because neither of the ions (positive or negative) is yet confined. As all of the above predicted observations are not found in these measurements, it is concluded that the dominant negative particle is the electron rather than the

negative ion. The saturation current in this case becomes [see also Eq. (13)]

$$\frac{I_{es}}{I_{+s}} = \sqrt{\frac{m_{H^+} \sum_{p=1 \dots} \frac{p n_{H_p^+}}{n_+}}{m_e}} \beta^*, \quad (14)$$

with p the number of atoms in an ion and $n_{H_p^+}$ the density of the H_p^+ ion. In Fig. 9 the calculated current ratios are given for $n_{H^+}/n_+ = 1$ and $n_{H_2^+}/n_+ = 1$. From these calculations it is possible to conclude that in the magnetized hydrogen plasma the dominant ion is H^+ . The arguments that were used to explain the results in nitrogen are also applicable to hydrogen. This result is therefore in agreement with the simple kinetic considerations explained in Sec. V.

VII. CONCLUSIONS

In the comparison of experiments to existing theory on the ratio of electron to ion saturation currents, the dependency on probe radius, as predicted by the theory, was not observed. Therefore the theory was used to derive an empirical formula that describes the ratio of electron saturation to ion saturation current. Under the assumption that this empirical formula remains valid in plasmas with a different composition, it was possible to derive relative ion densities in magnetized nitrogen and hydrogen plasmas.

ACKNOWLEDGMENTS

The authors thank M. J. F. van de Sande, A. B. M. Hüsken, and H. de Jong for their technical assistance. This work was supported by the Netherlands Technology Foundation (STW) and the Royal Netherlands Academy of Arts and Sciences (KNAW). This work is part of a collaborative effort between Wright Patterson Air Force Base and Eindhoven University of Technology and has been supported under the EOARD Contract No. SPC-95-4039.

-
- [1] M. J. de Graaf, R. J. Severens, L. J. van IJzendoorn, F. Munnik, H. J. M. Meijers, H. Kars, M. C. M. van de Sanden, and D. C. Schram, *Surf. Coat. Technol.* **74**, 351 (1995).
 - [2] R. J. Severens, G. J. H. Brussaard, M. C. M. van de Sanden, and D. C. Schram, *Appl. Phys. Lett.* **67**, 491 (1995).
 - [3] A. J. M. Buuron, M. C. M. van de Sanden, W. J. van Ooij, R. M. A. Driessens, and D. C. Schram, *J. Appl. Phys.* **78**, 528 (1995).
 - [4] A. J. M. Buuron, J. J. Beulens, P. Groot, J. Bakker, and D. C. Schram, *Thin Solid Films* **212**, 282 (1992).
 - [5] R. F. G. Meulenbroeks, R. A. H. Engeln, M. N. A. Beurskens, R. M. J. Paffen, M. C. M. van de Sanden, J. A. M. van der Mullen, and D. C. Schram, *Plasma Sources Sci. Technol.* **4**, 74 (1995).
 - [6] L. Schott, in *Plasma Diagnostics*, edited by W. Lochte-Holtgraven (North-Holland, Amsterdam 1968), Chap. 11.
 - [7] M. Bacal, G. W. Hamilton, A. M. Bruneteau, and H. J. Doucet, *Rev. Sci. Instrum.* **50**, 719 (1979).
 - [8] H. Mott-Smith and I. Langmuir, *Phys. Rev.* **28**, 727 (1926).
 - [9] J. G. Laframboise, University of Toronto, Institute for Aerospace Studies Report No. 100, 1966 (unpublished).
 - [10] D. Bohm, E. H. S. Burhop, and H. S. W. Massey: *The Characteristics of Electrical Discharges in Magnetic Fields*, edited by A. Guthrie and R. K. Wakering (McGraw-Hill, New York, 1949).
 - [11] R. J. Bickerton and A. von Engel, *Proc. Phys. Soc. London Sect. B* **69**, 468 (1956).
 - [12] J. R. Sanmartin, *Phys. Fluids* **13**, 103 (1970).
 - [13] T. Dote, H. Amemiya, and T. Ichimiya, *Jpn. J. Appl. Phys.* **3**, 789 (1964).
 - [14] E. O. Johnson and L. Malter, *Phys. Rev.* **80**, 58 (1950).
 - [15] R. P. Dahiya, M. J. de Graaf, R. J. Severens, H. Swelsen, M. C. M. van de Sanden, and D. C. Schram, *Phys. Plasmas* **1**, 2086 (1994).
 - [16] E. Graham, D. R. James, W. C. Keever, I. R. Gatland, D. L. Albritton, and E. W. McDaniel, *J. Chem. Phys.* **59**, 4648 (1973).
 - [17] H. Amemiya, *J. Phys. D* **23**, 999 (1990).